

Thermal modelling of high-power laser diodes mounted using various types of submounts

V.V. Bezotosnyi, O.N. Krokhin, V.A. Oleshchenko, V.F. Pevtsov, Yu.M. Popov, E.A. Cheshev

Abstract. Using three-dimensional thermal modelling of a high-power 980-nm laser diode with a stripe contact width of 100 μm as an example, we analyse the thermal parameters of high-power laser diodes mounted using submounts. We consider a range of thermal conductivities of submounts that includes parameters of widely used thermal compensators based on AlN, BeO and SiC, as well as on CuW and CuMo composites and polycrystalline and single-crystal synthetic diamond with high thermal conductivity. Taking into account experimental overall efficiency vs. pump current data, we calculate the temperature of the active layer as a function of the width, thickness and thermal conductivity of the submount at thermal loads corresponding to cw output powers of 10, 15 and 20 W.

Keywords: high-power laser diode, submount, efficiency, thermal management.

1. Introduction

In the past few years, advances in the fabrication of state-of-the-art high-power laser diodes have made it possible to overcome new technical and psychological limits in improving their output parameters. In particular, a laser diode with a stripe contact width of 100 μm has surpassed 50% efficiency and 10-W reliable output power levels. Even though available commercial high-power cw laser diodes are already capable of operating at extremely high thermal loads (heat flux densities in excess of 3 kW cm^{-2} can be removed from the active region), the possibilities of raising their output power are far from being exhausted. In a number of laboratories, work is under way to raise the reliable cw output power to 15–20 W [1–4]. The extremely high heat generation density in the active region of a high-power laser diode is due to the nanometre-scale thickness of the active layer in the laser heterostructure. Indeed, at a 50% overall efficiency, 10-W output power, 10-nm active layer thickness, 100- μm stripe contact width and 3-mm cavity length, the heat generation density exceeds 3 GW cm^{-3} , which is a record-high level for optoelectronic devices.

V.V. Bezotosnyi, O.N. Krokhin, Yu.M. Popov, E.A. Cheshev
P.N. Lebedev Physics Institute, Russian Academy of Sciences, Leninsky prosp. 53, 119991 Moscow, Russia; National Research Nuclear University MEPhI (Moscow Engineering Physics Institute), Kashirskoe sh. 31, 115409 Moscow, Russia; e-mail: victorbe@sci.lebedev.ru;
V.A. Oleshchenko, V.F. Pevtsov P.N. Lebedev Physics Institute, Russian Academy of Sciences, Leninsky prosp. 53, 119991 Moscow, Russia

Received 29 April 2014; revision received 26 May 2014
Kvantovaya Elektronika 44 (10) 899–902 (2014)
Translated by O.M. Tsarev

Given that, as shown earlier [4], raising the reliable output power to 20 W leads to a considerable decrease in overall efficiency, the thermal load on the heat spreader at this optical power is 30–35 W, and the heat flux density being removed increases to above 10 kW cm^{-2} . The removal of such continuous heat fluxes and, particularly, a substantial increase in them, necessary for further raising the output power at temperature differences near 30°C relative to the temperature of the basic heat sink, permissible for ensuring reliable operation of the semiconductor crystal, require novel, more effective approaches, technologies and materials.

In addition to thermal management, the technology of high-power laser diodes poses another fundamental problem, arising from the significant differences in thermal and mechanical properties between semiconductor and heat-sink materials: the problem of thermoelastic stress in hybrid structures of mounted high-power diode lasers.

In most instances, the problem of thermoelastic stress can be solved using so-called thermal compensators in the form of a crystalline, ceramic or composite layer between a basic copper heat sink and the semiconductor laser crystal. Thermal compensators most frequently encountered in state-of-the-art structures consist of AlN, BeO and SiC, as well as of CuW and CuMo composites. The thermal compensators from these materials differ little in thermal expansion coefficient from the semiconductor. Their drawback is that their thermal conductivity, 150–250 $\text{W m}^{-1} \text{K}^{-1}$, is considerably lower than that of copper. The most advanced composite material so far is copper–diamond, developed at Sumitomo Electric (Japan), with thermal conductivity as high as 1000 $\text{W m}^{-1} \text{K}^{-1}$, but submounts from this material for laser diodes have a number of drawbacks. In addition to the rather high cost of such components, there are difficulties pertaining to the fabrication process, namely, to the limitations on the smallest grain size of the composite. This parameter limits their potential from the viewpoint of heat transfer efficiency, in particular, that related to the working surface roughness limit and working edge geometry.

2. Thermal modelling

The thermal modelling of an assembly in the form of a hybrid structure comprising a semiconductor laser crystal, a basic copper heat sink and an intermediate heat sink is of considerable practical interest. As shown below, the results of such modelling with COMSOL software make it possible to gain insight into the fundamental nature of the efficiency of such structures as a function of the thermal load, the geometric parameters and thermal conductivity of their elements and boundary conditions. Three-dimensional (3D) thermal mod-

elling offers the possibility of varying the above parameters and optimising the design of hybrid structures at a given output power level and required material parameters.

In thermal modelling, we used parameters of a single high-power 980-nm laser diode (LD) with a stripe contact width of 100 μm , mounted on a copper heat sink of the C-mount type, without submounts. The exceptionally large emission parameters of such LDs are due to the use of asymmetric broad-waveguide heterostructures [5–7]. Figure 1 shows an experimental light power–current ($L-I$) curve obtained for an LD by short-term measurements in continuous mode.

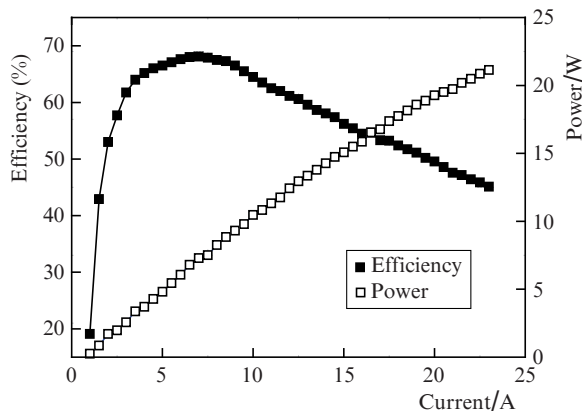


Figure 1. Experimental light power–current curve and overall efficiency as a function of pump current for a single 980-nm laser diode with a stripe contact width of 100 μm .

The maximum power was about 22 W, the slope of the $L-I$ curve was 1.1 W A^{-1} , and the maximum overall efficiency was as high as 68%. It is seen that the maximum in efficiency takes place at pump currents near 7 A. At higher diode currents, the efficiency drops significantly because of the rather high series resistance of the laser diode. From this point of view, the ability to reduce the series resistance is of great practical interest, because this would ensure an increase in overall efficiency and reliable output power. To resolve this issue, it is necessary to optimise the laser heterostructure design, in particular the height of the heterobarriers and the thickness of the waveguide layers and wide-band-gap emitters, and doping.

The above experimental data were used as basic in modelling the parameters of such laser crystals mounted on a copper heat sink of the F-mount type, more efficient in comparison with C-mounts, using various types of submounts. Our purpose was to calculate the cavity-average temperature of the active layer along the length of the laser crystal while varying the main parameters of the submount – thickness, width and thermal conductivity – at various thermal loads.

Figure 2 shows calculated temperature distributions for the above hybrid design at a thermal load of 30 W, with a diamond submount having a thermal conductivity of 1200 $\text{W m}^{-1} \text{K}^{-1}$, typical of synthetic polycrystalline diamond grown by plasma CVD and utilised in previous experimental studies [8–10]. The thermal modelling of laser diodes has been the subject of extensive research, including Refs [11–16], but to the best of our knowledge detailed 3D modelling of high-power laser diodes at varied parameters of different types of submounts is presented in this report for the first time.

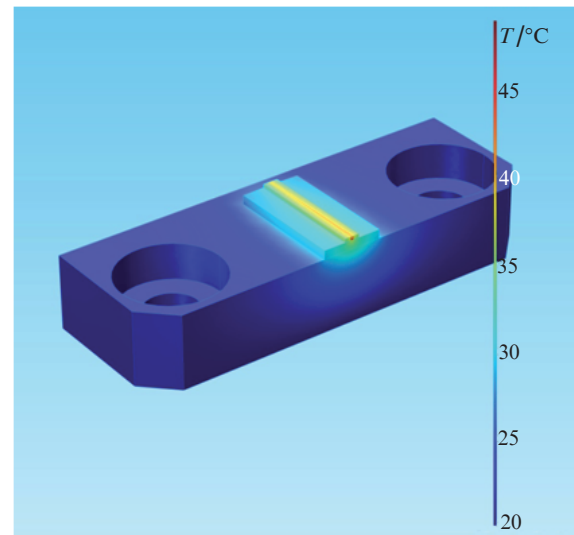


Figure 2. Temperature distribution in a hybrid laser diode structure with a diamond submount (thermal conductivity of 1200 $\text{W m}^{-1} \text{K}^{-1}$) and a basic heat sink of the F-mount type at a thermal load of 30 W.

In our calculations, we used the minimum technologically feasible dimensions of the diamond submount, corresponding to its minimum cost: 0.3 mm thickness and 3 mm width. It is seen that, when the temperature of the lower basal plane of the F-mount is 20°C, the temperature at the output mirror considerably increases, reaching 49°C. This temperature approaches the reliable operation limit (according to our experimental data, the maximum temperature difference for reliable operation should not exceed 30°C with respect to the 20°C basic level [4]).

Figure 3 shows the average temperature of the active layer at thermal loads of 10, 20 and 30 W. The hybrid structure under consideration comprises a laser crystal, a submount and a basic heat sink of the F-mount type, which ensures heat removal considerably more uniform over the working surface and more efficient than do C-mounts. The thickness of the F-mount used in our calculations (2.5 mm) corresponded to a standard design, and the material of the F-mount was copper, with a thermal conductivity of 400 $\text{W m}^{-1} \text{K}^{-1}$. As a boundary condition, the temperature of the lower basal plane of the copper F-mount was taken to be constant at 20°C, which corresponded to the experimental conditions of this study, because a temperature sensor of the thermal stabilisation system was located on that surface.

The width, thickness and thermal conductivity of the submount were varied from 3 to 6 mm, from 0.1 to 0.8 mm and from 100 to 2400 $\text{W m}^{-1} \text{K}^{-1}$, respectively. These ranges correspond to submount materials of technological and practical interest: from composites with a thermal conductivity between 150 and 250 $\text{W m}^{-1} \text{K}^{-1}$ to high-quality diamond single crystals with a thermal conductivity of up to 2400 $\text{W m}^{-1} \text{K}^{-1}$.

Comparison of the results in Figs 3a–3c leads us to the following conclusions:

1. The maximum temperature increases from 50°C at a thermal load of 10 W to 113°C at a thermal load of 30 W (the thickness and width of the submount are 0.1 and 3 mm).
2. As would be expected, at thermal conductivities of submounts from 100 to 400 $\text{W m}^{-1} \text{K}^{-1}$ the temperature of the active layer depends most strongly on the thickness of the

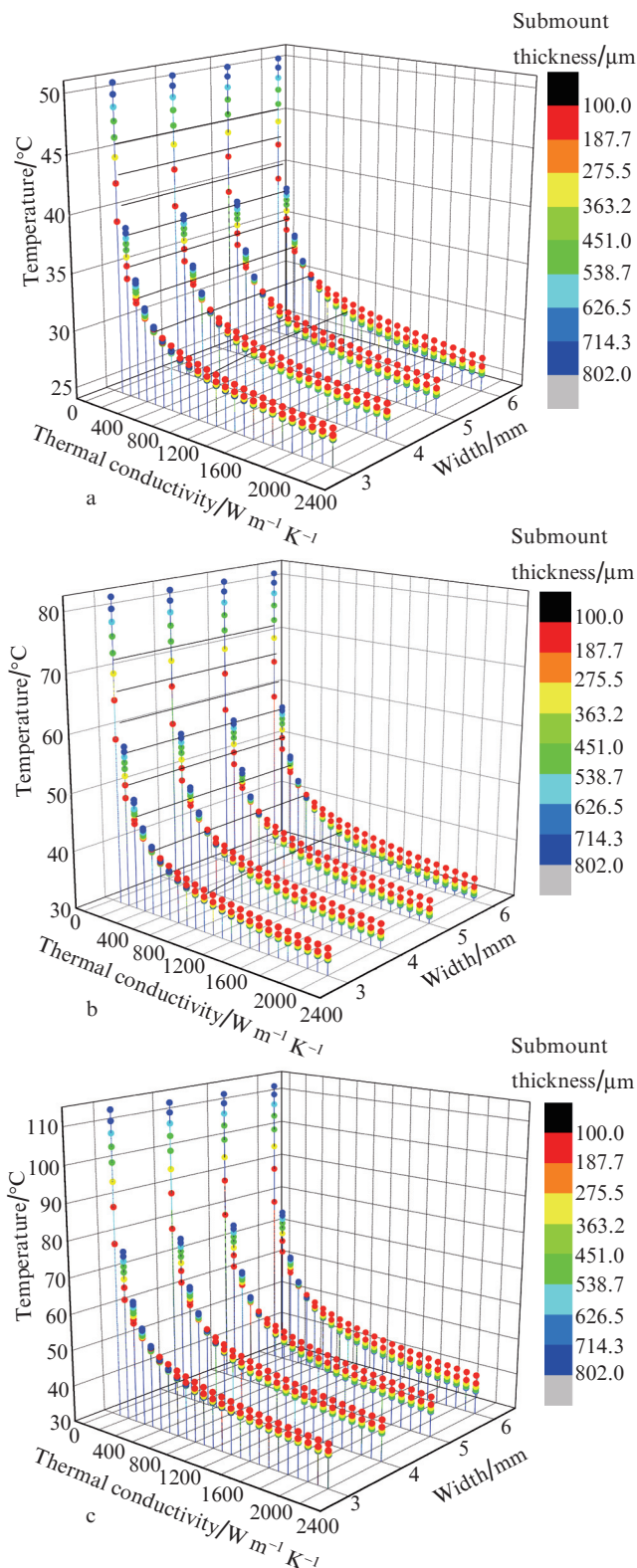


Figure 3. Average temperature of the active layer of a laser diode at a thermal load of (a) 10, (b) 20 and (c) 30 W against the thickness, width and thermal conductivity of a submount on a basic heat sink of the F-mount type. The thickness of the submount is specified on the right-hand scale.

submount: at a thickness of 0.1 mm and thermal load of 30 W, the temperature increases from 76 to 113 °C.

3. As the thermal conductivity of the submount increases, the effect of its thickness on the temperature of the active

layer decreases. When the thermal conductivity increases to above 400 W m⁻¹ K⁻¹ (the thermal conductivity of the basic copper F-mount), the results for various thicknesses of the submount 'merge'. Note that the point where this occurs corresponds to a slightly higher thermal conductivity, which is obviously related to the additional increase in the thermal resistance of the entire structure because of the increase in the total thickness of the heat-spreading components.

4. At a thermal conductivity above that of the basic F-mount, increasing the thickness of the submount reduces the temperature of the active layer, as would be expected. The effect becomes stronger with an increase in the thermal conductivity and width of the submount. In particular, at a thermal load of 30 W and thermal conductivity of 1600 W m⁻¹ K⁻¹, the change in the temperature of the active layer at thicknesses in the range 0.1–0.8 mm increases from 3 °C at a width of 3 mm to 6 °C at a width of 6 mm.

5. At lower thermal loads, the distinctions between the above dependences are substantially smaller. In particular, at a thermal load of 10 W and thermal conductivity of 1600 W m⁻¹ K⁻¹, the corresponding temperature change is 1.5–3 °C.

The dependences of the temperature of the active layer on the thermal conductivity of the submount are rather interesting. The present results demonstrate that, from a practical point of view, at a thermal conductivity above 1600 W m⁻¹ K⁻¹ the temperature decreases insignificantly, so it is unreasonable to increase the thermal conductivity. This result is important for modern synthetic diamond growth technology because 1200 W m⁻¹ K⁻¹ lies between typical thermal conductivities of polycrystalline and single-crystal synthetic diamond materials. At present, the growth of single-crystal diamond is much more complex and, accordingly, more expensive than the preparation of polycrystalline diamond, so polycrystalline wafers, in particular those grown by plasma CVD, are considerably larger and cheaper.

In this context, the dependences of the active-layer temperature on the thickness and width of the submount are of interest. The geometric dimensions of the submount should primarily ensure a sufficiently effective cooling of the laser crystal, but at the same time they should be minimised in order to reduce the cost of the submount, which is particularly critical for expensive diamond materials.

On the whole, the results presented in Fig. 3 provide sufficient information for optimising both submounts with high thermal conductivity and thermal compensators with a thermal conductivity lower than that of copper. These results can be used to improve the effectiveness of heat removal not only from high-power laser diodes but also from other types of high-energy electronic and optoelectronic components with high heat generation localisation, i.e. they have a rather extensive application area and are of methodological importance.

3. Conclusions

Using a single high-power 980-nm laser diode with a stripe contact width of 100 μm as an example, we have obtained 3D plots of the active-layer temperature against basic parameters of submounts – width, thickness and thermal conductivity – at thermal loads corresponding to output powers of 10, 15 and 20 W, with allowance for the maximum overall efficiency, the type of basic copper heat sink and boundary conditions. The present results enable the parameters of essentially all types of submounts in use or under development to be opti-

mised in terms of effective heat removal and cost at various laser output powers and thermal loads. Using the modelling data obtained, for every type of basic heat sink one can determine the limiting reliable output power in the case of thermal compensators with a thermal conductivity lower than that of copper and optimise the high-power laser diode design with the aim of reaching reliable output powers in the range 10–20 W using synthetic diamond submounts with various geometries and high thermal conductivity.

Acknowledgements. This work was supported by the Russian Foundation for Basic Research (Grant No. 14-02-31718 mol_a) and the Physical Sciences Division of the Russian Academy of Sciences (Programme No. 7OFN).

References

1. Crump P., Blume G., Paschke K., Staske R., Pietrzak A., Zeimer U., Einfeldt S., Ginolas A., Bugge F., Häusler K., Ressel P., Wenzel H., Erbert G. *Proc. SPIE Int. Soc. Opt. Eng.*, **7198**, 719814-1 (2012).
2. Sin Yongkun, LaLumondiere Stephen D., Presser Nathan, Foran Brendan J., Ives Neil A., Lotshaw William T., Moss Steven C. *Proc. SPIE Int. Soc. Opt. Eng.*, **8241**, 824116-1 (2012).
3. Yanson Dan, Cohen Shalom, Levy Moshe, Shamay Moshe, Geva ara, Berk Yuri, Tesler Renana, Klumel Genadi, Rappaport Noam, Karni Yoram. TuP13 (Contributed Poster), 978-1-4577-0829-9/12/ 2012, IEEE.
4. Bezotosnyi V.V., Krokhin O.N., Oleshchenko V.A., Pevtsov V.F., Popov Yu.M., Cheshev E.A. *Kvantovaya Elektron.*, **44** (2), 145 (2014) [*Quantum Electron.*, **44** (2), 145 (2014)].
5. Vinokurov D.A., Zorina S.A., Kapitonov V.A., Murashova A.V., Nikolaev D.N., Stankevich A.L., Khomylev M.A., Shamakhov V.V., Leshko A.Yu., Lyutetskii A.V., Nalet T.A., Pikhtin N.A., Slipchenko S.O., Sokolova Z.N., Fetisova N.V., Tarasov I.S. *Fiz. Tekh. Poluprovodn.*, **39** (3), 388 (2005).
6. Andreev A.Yu., Leshko A.Yu., Lyutetskii A.V., Marmalyuk A.A., Nalet T.A., Padalitsa A.A., Pikhtin N.A., Sabitov D.R., Simakov V.A., Slipchenko S.O., Khomylev M.A., Tarasov I.S. *Fiz. Tekh. Poluprovodn.*, **40** (5), 628 (2006).
7. Vinokurov D.A., Stankevich A.L., Shamakhov V.V., Kapitonov V.A., Leshko A.Yu., Lyutetskii A.V., Nikolaev D.N., Pikhtin N.A., Rudova N.A., Sokolova Z.N., Slipchenko S.O., Khomylev M.A., Tarasov I.S. *Fiz. Tekh. Poluprovodn.*, **40** (6), 764 (2006).
8. Ashkinazi E.E., Bezotosnyi V.V., Bondarev V.Yu., Kovalenko V.I., Krokhin O.N., Oleshchenko V.A., Pevtsov V.F., Popov Yu.M., Cheshev E.A. *Trudy konf. 'Poluprovodnikovye lazery i sistemy'* (Proc. Conf. Semiconductor Lasers and Systems) (Minsk, 2011) p. 29.
9. Ashkinazi E.E., Bezotosnyi V.V., Bondarev V.Yu., Kovalenko V.I., Konov V.I., Krokhin O.N., Oleshchenko V.A., Pevtsov V.F., Popov Yu.M., Popovich A.F., Ral'chenko V.G., Cheshev E.A. *Kvantovaya Elektron.*, **42** (11), 959 (2012) [*Quantum Electron.*, **42** (11), 959 (2012)].
10. Bezotosnyi V.V., Bondarev V.Yu., Krokhin O.N., Oleshchenko V.A., Pevtsov V.F., Popov Yu.M., Cheshev E.A. *Tez. dokl. simp. 'Poluprovodnikovye lazery: fizika i tekhnologiya'* (Abstracts Symp. Semiconductor Lasers: Physics and Technology) (St. Petersburg, 2012) p. 14.
11. Nakwaski W. *Int. J. Optoelectron.*, **5** (5), 451 (1990).
12. Nakwaski W. *IEE Proc. I*, **131** (3), 94 (1984).
13. Nakwaski W. *Kvantovaya Elektron.*, **11** (2), 391 (1984) [*Sov. J. Quantum Electron.*, **14** (2), 266 (1984)].
14. Bezotosnyi V.V., Kumykov Kh.Kh., Markova N.V. *Kvantovaya Elektron.*, **23** (9), 775 (1996) [*Quantum Electron.*, **26** (9), 755 (1996)].
15. Bezotosnyi V.V., Kumykov Kh.Kh. *Kvantovaya Elektron.*, **25** (3), 225 (1998) [*Quantum Electron.*, **28** (3), 217 (1998)].
16. Ter-Martirosyan A.L., Demidov D.M., Sverdlov M.A., Kulik A.V., Karpov S.Yu. *Nauchn. Priborost.*, **23** (4), 45 (2013).